

## Positive Domain Wall Resistance of 180° Néel Walls in Co Thin Films

Dieter Buntinx,\* Steven Brems, Alexander Volodin, Kristiaan Temst, and Chris Van Haesendonck

*Laboratorium voor Vaste-Stoffysica en Magnetisme, Katholieke Universiteit Leuven, Celestijnenlaan 200 D, B-3001 Leuven, Belgium*

(Received 17 February 2004; published 11 January 2005)

We measured the intrinsic domain wall resistance (DWR) of 180° Néel walls in a polycrystalline Co thin film deposited on top of a patterned antiferromagnetic CoO template. After field cooling through the CoO blocking temperature, exchange bias induces a spatially modulated coercivity of the Co film, resulting in a periodic domain pattern with 180° Néel walls. The intrinsic DWR is determined unambiguously by using rotating magnetic fields that result in a reversible creation and annihilation of the Néel walls. In contrast with earlier reports, the DWR is positive and in agreement with models based on the giant magnetoresistance mechanism. A reliable, quantitative determination of the DWR requires careful numerical evaluation of the anisotropic magnetoresistance effect.

DOI: 10.1103/PhysRevLett.94.017204

PACS numbers: 75.60.Ch, 75.30.Gw, 75.47.-m

The intrinsic effect of domain walls on the resistance of ferromagnetic metals has been studied intensively during recent years. Relying on the influence of shape anisotropy, crystalline anisotropy or a combination of both to tailor the ferromagnetic domain structure, domain wall resistance (DWR) was identified in several ferromagnetic thin films. The experiments led, however, to conflicting observations, where domain walls either increase (positive DWR) or decrease (negative DWR) the resistance. Bloch-like domain walls, where the magnetization inside the domain wall rotates out of the plane determined by the magnetization and the measuring current, were investigated in detail. Positive DWR was observed in NiFe-Gd-NiFe trilayers [1], epitaxial FePd nanostructures [2], hcp Co thin films [3], and in the metallic perovskite SrRuO<sub>3</sub> [4], while a negative contribution was found in epitaxial Fe wires [5,6]. For the case where the magnetization inside the domain wall rotates in the film plane, i.e., for Néel walls, very few observations exist. Unlike for a Bloch wall, it is not possible to avoid for a Néel wall the presence of an anisotropic magnetoresistance (AMR) contribution by an appropriate sample design. A quantitative assessment of the AMR contribution is therefore essential when determining the DWR of Néel walls. In previous measurements the resistance of Néel-type domain walls was investigated in Co zigzag wires [7] and in cross-shaped NiFe junctions [8]. Because of the different magnetic spin configuration of these shape anisotropy induced domain walls when compared to standard domain walls, a reliable quantitative determination of the intrinsic domain wall resistance is not possible.

In this Letter, we report on the successful creation of well-defined 180° Néel domain walls in a continuous ferromagnetic polycrystalline Co thin film by bringing the Co in contact with a stripe pattern defined in an antiferromagnetic, insulating CoO film. By applying a rotating magnetic field we are able to reversibly create and remove the Néel walls. This enables an unambiguous, quantitative determination of the DWR of 180° Néel walls in a poly-

crystalline Co film. We note a comparable method with patterned exchange-spring bilayers was used before to investigate DWR [9]. In these experiments, the parallel electrical conduction in the two layers does, however, not allow a quantitative analysis of the intrinsic DWR.

In previous experiments the direct experimental observation of DWR has been hindered by the various magnetoresistance effects that are present in ferromagnetic metals. Three magnetoresistance contributions have to be considered: (i) the Lorentz magnetoresistance originating from the deflection of the current lines inside magnetic domains, (ii) the well-known anisotropic magnetoresistance effect [10] originating from the spin-orbit coupling, and (iii) the magnetoresistance effect linked to the wiggling of the current lines at the domain walls [11]. Because of the polycrystalline character of our films, the mobility of the electrons is rather low and the product of the cyclotron frequency and the relaxation time  $\omega_c \tau \ll 1$ . Therefore, the Lorentz effect and the wiggling effect can be neglected, since the time between two consecutive scattering events is not sufficient to curve the trajectory of the electrons. For the AMR effect, a reliable quantitative assessment of its contribution to the measured resistance is possible, as shown below.

Our method to control the creation of the domain walls is based on the exchange bias effect [12] in CoO/Co bilayers. Cooling such a bilayer below the Néel temperature of the antiferromagnetic CoO ( $T_N \approx 290$  K) in the presence of a magnetic field results in a negative shift of the hysteresis loop of the ferromagnetic Co. The biased Co behaves as if it possesses a unidirectional anisotropy axis along the cooling field direction. The loop shift is referred to as the exchange bias field  $H_{eb}$ . In CoO/Co thin film systems  $H_{eb}$  vanishes at the blocking temperature ( $T_B$ ), which is below the Néel temperature. By locally biasing a Co thin film, the coercive fields can be altered at specific positions and domain structures can be imposed by the application of well-defined magnetic fields.

Local biasing is introduced in a continuous Co film grown on top of a patterned CoO layer consisting of  $2\ \mu\text{m}$  wide stripes repeated with a  $15\ \mu\text{m}$  period. The stripes are fabricated by a combination of UV lithography and lift-off techniques. The CoO is formed by the *in situ* oxidation (in a pure oxygen atmosphere of  $10^{-3}$  mbar) of a  $2\ \text{nm}$  thick, sputtered Co film. The resulting CoO stripes have a thickness of 3 to 4 nm. The deposition of the continuous Co film on top of the stripes is performed by molecular beam epitaxy. Since the exchange bias effect nucleates at the interface between the ferromagnet and the antiferromagnet, it is important to have a clean CoO surface. To remove any contamination resulting from the lift-off, the stripes are annealed at a temperature of  $250\ ^\circ\text{C}$  before a  $20\ \text{nm}$  Co layer is deposited. Finally, the sample is covered with a  $3\ \text{nm}$  Au capping layer to prevent oxidation. Figure 1(a) shows a schematic drawing of the patterned bilayer.

The properties of the patterned CoO/Co bilayer are studied by magnetization measurements and four-point magnetoresistance measurements. Magnetization loops at low temperature are obtained with a vibrating sample magnetometer. To measure the magnetoresistance, a  $100\ \mu\text{m}$  wide and  $1\ \text{mm}$  long four-terminal resistance pattern containing 68 CoO stripes is dry etched in the bilayer. By connecting the four-terminal pattern to an Adler-Jackson bridge and using a lock-in amplifier, the magnetoresistance can be determined with high sensitivity.

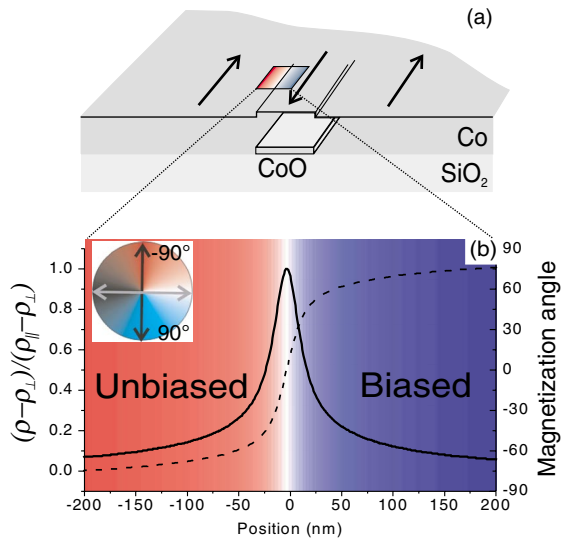


FIG. 1 (color). (a) Schematic drawing of the patterned bilayer. A continuous Co film is deposited on top of  $2\ \mu\text{m}$  wide CoO stripes. After field cooling the Co film is locally exchange biased and the stripe domain pattern can be created by reversing the magnetic field. The color contrast and the dotted line in (b) represent the changing magnetization direction with respect to the current inside the Néel wall, which is obtained from micromagnetic simulations. The continuous line gives the corresponding calculated AMR resistivity inside the wall.

The ac measuring current has a frequency of  $27.7\ \text{Hz}$ , a root-mean-square (rms) amplitude of  $3.5\ \mu\text{A}$  and is directed perpendicular to the CoO stripes. The resistance of the four-terminal pattern at  $5\ \text{K}$  is  $29.7\ \Omega$ .

In order to create a stripe domain pattern, the sample is field cooled below its blocking temperature ( $T_B \approx 120\ \text{K}$ ) in a direction parallel to the CoO stripes. The parts in between the stripes (unbiased regions) act like a normal Co thin film, while the parts on top of the stripes (biased regions) feel an additional exchange bias field. In the presence of a magnetic field, both the biased and unbiased regions have a saturated magnetization and no domain walls are present. Upon decreasing and reversing the field, the unbiased regions reverse their magnetization first, creating magnetic domains separated by  $180^\circ$  domain walls [see the arrows in Fig. 1(a)]. This domain configuration remains stable until the magnetic field exceeds the exchange bias field of the biased regions and the complete Co film is saturated in the opposite direction. Figure 2(a) shows two consecutive magnetic hysteresis loops that are measured after cooling to  $5\ \text{K}$  in a field of  $400\ \text{mT}$  parallel

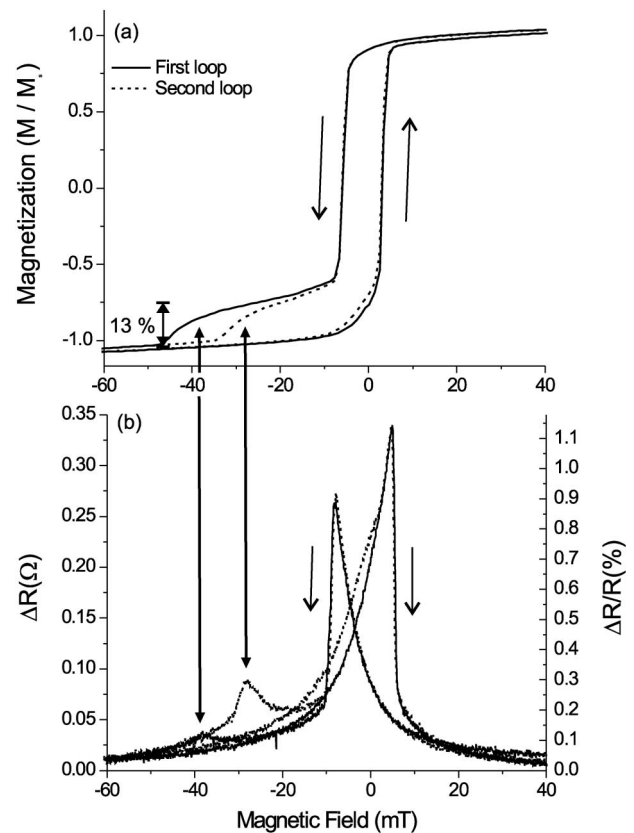


FIG. 2. Magnetization (a) and magnetoresistance (b) at  $5\ \text{K}$  of the patterned CoO/Co bilayer for two consecutive hysteresis loops with the field parallel to the CoO stripes. The sample was cooled from room temperature in a field of  $400\ \text{mT}$  parallel to the stripes. The two-step behavior of the magnetization loop and the smaller peaks in the magnetoresistance confirm the presence of the stripe domain pattern.

to the CoO stripes. Identical field cooling conditions are used for all measurements reported in this Letter. When lowering the field, a clear two-step behavior becomes visible in both loops, confirming the existence of the stripe domain pattern. After the first step approximately 13% of the magnetization remains to be reversed, in nice agreement with the covering fraction  $2/15 = 0.133$  for the CoO stripes. The reversal of the biased regions during the second step takes place at different magnetic fields for the two consecutive loops. This can be explained by the training effect [13] in CoO/Co exchange bias systems. The first reversal of a biased film occurs by domain wall nucleation and domain wall motion, while all subsequent reversals are dominated by spin rotation. Consequently, the coercive field decreases after the first reversal. For positive fields the biased and unbiased regions reverse almost simultaneously.

Figure 2(b) shows the results for the corresponding magnetoresistance. At negative fields both magnetoresistance measurements show two distinctive peaks, while at positive fields only one peak is present. The peaks originate from the AMR effect, which is the dominating source of magnetoresistance in ferromagnets. The AMR effect depends on the angle between the current and the magnetization and reaches a maximum resistivity  $\rho_{\parallel}$  (minimum resistivity  $\rho_{\perp}$ ) for a parallel (perpendicular) arrangement. An increase in the resistance in Fig. 2(b) corresponds to a deviation of the magnetization direction from the cooling field direction, i.e., rotation of the magnetic moments. The first peak at negative fields reflects the reversal of the unbiased regions. When further decreasing the field, a second smaller peak corresponds to the reversal of the biased regions. In the second measurement the height of this peak is enhanced because of the additional spin rotation resulting from the training effect. These results show that magnetoresistance measurements are a valuable alternative tool to distinguish between the different magnetization reversal processes.

For both loops there exists a well-defined field region between  $-10$  and  $-20$  mT where only the unbiased regions are reversed, i.e., where the stripe domain pattern is present. In principle, the resistance of the domain walls can be determined by comparing the resistance in this field region to the resistance in a field region where no domain walls are present. However, it is very difficult to extract this information because of an unknown mixing between the AMR resistance and the DWR.

In our experiments, the DWR of the  $180^{\circ}$  domain walls is determined with a rotating magnetic field as shown in Fig. 3. The sample is field cooled and training is completed by performing two consecutive loops. After applying a saturating field of 100 mT in the cooling field direction, the magnetic field is lowered to 16.9 mT. At this field value the biased as well as the unbiased regions are still saturated [Fig. 3(a)]. Because all the magnetic moments are perpen-

dicular to the current, the corresponding AMR reaches a minimum. Next, the magnetic field with constant magnitude is rotated over  $360^{\circ}$  in the plane of the film, while the magnetoresistance is monitored. During the rotation the field is sufficiently large to ensure a perfect alignment of the magnetization of the unbiased regions with the external field. In the biased regions, however, the exchange bias field keeps the magnetization aligned within  $20^{\circ}$  along the direction of the cooling field.

Combining the biased and the unbiased field response, the following magnetization rotation cycle occurs. Rotating from  $0^{\circ}$  to  $90^{\circ}$  [Fig. 3(b)], the magnetization in between the stripes follows the magnetic field, causing a gradual increase of the resistance, while the magnetization direction of the biased regions does not change considerably. When further rotating the field, the stripe domain pattern is achieved at  $180^{\circ}$  [Fig. 3(c)]. The unbiased and biased regions are aligned parallel and antiparallel to the external field, respectively. Continuing the rotation, a state

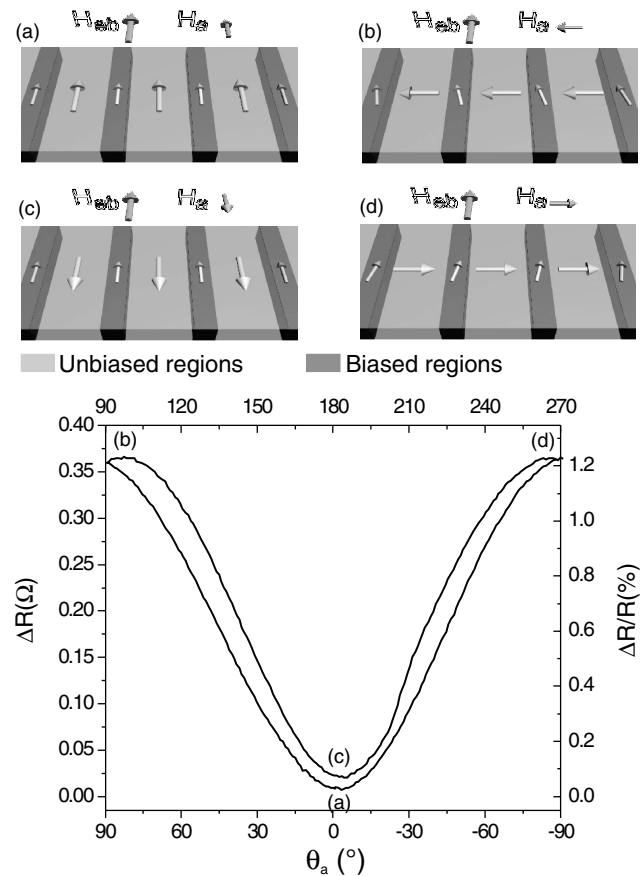


FIG. 3. Variation of the magnetoresistance (with respect to the resistance  $R$  at 100 mT) when rotating a magnetic field with a magnitude of 16.9 mT in the plane of the patterned CoO/Co. The bottom and the top axis refer to the bottom and the top curve, respectively. The labels (a)–(d) correspond to the diagrams in the upper panels. The artificial stripe domain pattern is created at an angle of  $180^{\circ}$  (c).

identical to the  $90^\circ$  state is found at  $270^\circ$  [Fig. 3(d)]. Finally, the loop is closed at  $360^\circ$  where the system returns to its initial magnetic state.

An important advantage of this technique is that formation of the domain walls occurs in a very controlled way. The reduced film thickness ensures that only the creation of Néel walls is possible [14]. In addition, the rotation of magnetic moments inside the domain walls is fixed by the rotation direction of the external magnetic field. By rotating the field anticlockwise, the walls at the right-hand side of the CoO stripes will have a clockwise rotation, while the left-hand side walls have an anticlockwise rotation. Also, the domain walls retain their rotation direction over the complete sample width; i.e., our technique makes the controlled creation of Néel walls possible. In addition, the presence of the Néel walls was confirmed by low temperature magnetic force microscopy [15].

Our measurements reveal a clear difference in resistance between the initial state and the antiparallel state, a difference that can be linked to the appearance of the domain walls. Analyzing several measurements and taking into account a total number of 136 domain walls, we find an average resistance increase of  $76.4 \pm 0.7 \mu\Omega$  per domain wall. The question is then whether the observed resistance increase is intrinsic for the domain walls or whether it can be explained by the AMR effect present in our ferromagnetic thin films. In contrast to Bloch walls, the angle between the current and the magnetization cannot be kept constant inside a Néel wall and part of the DWR will be a result of the AMR effect. We developed a computational model based on micromagnetic simulations [16] to calculate the contribution of the AMR effect. This model was successfully used before to simulate the AMR in ferromagnetic ring structures [17], where it was possible to reproduce the experimental results within a few percent without the use of any free fitting parameters.

The stripe domain pattern can be reproduced by micromagnetic simulations for which we use a cell size of only 1 nm. The exchange bias effect is accounted for by adding an additional internal magnetic field to the biased regions of the ferromagnet. The additional internal field leads to an asymmetry of the domain wall, but the simulations indicate that this asymmetry is very small. The resulting color contrast in Fig. 1(b) clearly reveals the presence of a Néel wall in between the two regions of opposite magnetization. The width of the domain wall inferred from the simulations is about 60 nm. The line profile in Fig. 1(b) shows the calculated normalized AMR resistivity inside the simulated Néel wall. Relying on this result, the total resistance due to the AMR effect can be calculated from the parameters obtained from the reference film ( $\rho_{\parallel} - \rho_{\perp} = 8.75 \times 10^{-10} \Omega\text{m}$ ). We find that the AMR contribution cannot exceed  $44.5 \mu\Omega$  for a single domain wall. Correcting for the AMR effect and multiplying by the width and the thickness of the resistance path, an intrinsic

positive interface resistance of  $6.4 \times 10^{-17} \Omega\text{m}^2$  is found for the Néel walls. This agrees with the results obtained for continuous Co films containing  $180^\circ$  Bloch walls [3]. The positive domain wall resistance of the Néel walls can be explained by the model of Levy *et al.* [18], which relies on the giant magnetoresistance mechanism. For uniform magnetization, one of the two spin channels has a much lower resistivity and short circuits the other spin channel. A change in the magnetization direction in a domain wall leads to mixing of the two spin channels and results in an increased resistivity. Our results can be explained assuming a spin mixing coefficient of about 65, which is higher than for ferromagnetic thin films in the absence of exchange bias [18].

In conclusion, we are able to induce  $180^\circ$  Néel walls in a controllable and reversible way. The domain wall resistance of such domain walls can be determined quantitatively and unambiguously. The wall resistance is positive and can be understood in terms of the giant magnetoresistance effect. Further investigations of the domain wall resistance are under way for alternative antiferromagnetic templates, enabling one to create different domain patterns.

This work has been supported by the Fund for Scientific Research–Flanders (FWO) as well as by the Flemish Concerted Action (GOA) and the Belgian Interuniversity Attraction Poles (IAP) research programs. The authors thank J. Bekaert, I. Gordon, M. Malfait, B. Opperdoes, and J. Swerts for their help with the experiments.

---

\*Electronic address: dieter.buntinx@fys.kuleuven.ac.be

- [1] J.L. Prieto, M.G. Blamire, and J.E. Evetts, *Phys. Rev. Lett.* **90**, 027201 (2003).
- [2] R. Danneau *et al.*, *Phys. Rev. Lett.* **88**, 157201 (2002).
- [3] J.F. Gregg *et al.*, *Phys. Rev. Lett.* **77**, 1580 (1996).
- [4] L. Klein *et al.*, *Phys. Rev. Lett.* **84**, 6090 (2000).
- [5] U. Ruediger *et al.*, *Phys. Rev. Lett.* **80**, 5639 (1998).
- [6] A.D. Kent *et al.*, *J. Phys. Condens. Matter* **13**, R461 (2001).
- [7] T. Taniyama *et al.*, *Phys. Rev. Lett.* **82**, 2780 (1999).
- [8] Y.B. Xu *et al.*, *Phys. Rev. B* **61**, 14 901 (2000).
- [9] T. Nagahama, K. Mibu, and T. Shinjo, *J. Appl. Phys.* **87**, 5648 (2000).
- [10] I.A. Campbell and A. Fert, in *Ferromagnetic Materials*, edited by E.P. Wohlfarth (North-Holland, Amsterdam, 1982), Vol. 3; T.R. McGuire and R.I. Potter, *IEEE Trans. Magn.* **11**, 1018 (1975).
- [11] L. Berger, *J. Appl. Phys.* **49**, 2156 (1978).
- [12] W.H. Meiklejohn and C.P. Bean, *Phys. Rev.* **102**, 1413 (1956).
- [13] F. Radu *et al.*, *Phys. Rev. B* **67**, 134409 (2003).
- [14] B.A. Lilley, *Philos. Mag.* **41**, 792 (1950).
- [15] A. Volodin *et al.* (unpublished).
- [16] The object oriented micromagnetic framework is available at <http://math.nist.gov/oommf>.
- [17] D. Buntinx *et al.*, *Phys. Rev. B* **70**, 224405 (2004).
- [18] P.M. Levy and S. Zhang, *Phys. Rev. Lett.* **79**, 5110 (1997).